Supplementary Materials for

Activation mechanism of a human SK-calmodulin channel complex elucidated by cryo-EM structures

Chia-Hsueh Lee, Roderick MacKinnon*

Affiliations:

Laboratory of Molecular Neurobiology and Biophysics, The Rockefeller University, Howard Hughes Medical Institute, 1230 York Avenue, New York, New York 10065, USA.

*Correspondence to: mackinn@rockefeller.edu

This PDF file includes:

Other Supplementary Materials for this manuscript includes the following:

Supplementary Materials:

Materials and Methods

Figs S1 to S8

Table S1

Movie S1

References (*62-80*)

Materials and Methods

Construct design

DNA segments encoding SK channels were synthesized and cloned into the pEG BacMam vector (*62*), where each SK gene is placed before a PreScission protease cleavage site, followed by a C-terminal green fluorescent protein (GFP) tag. These constructs were screened by FSEC (*20*), from which the human SK4 channel was identified. The expression cassette containing human SK4 (including the GFP-tag) or human CaM was amplified, and these two cassettes were assembled into the pBIG1a vector using biGBac method (*63*). This multigene expression construct of the SK4/CaM complex was used for large-scale protein expression.

Protein Expression and purification

The SK/CaM complex was expressed in HEK293S GnTI$^-$ cells using the BacMam method (*62*). Briefly, a bacmid carrying the complex was generated by transforming *E. coli* DH10Bac cells with the SK4/CaM complex construct according to the manufacturer's instructions (Bac-to-Bac; Invitrogen). Baculoviruses were produced by transfecting Sf9 cells with the bacmid using Cellfectin II (Invitrogen). After two rounds of amplification, baculoviruses were used for cell transduction. Suspension cultures of HEK293S GnTI$^-$ cells were grown at 37 °C to a density of ~3 x 10^6 cells/ml and viruses were added (12% v/v) to initiate the transduction. After 10–12 h, 10 mM sodium butyrate was supplemented and the temperature was shifted to 30 °C. Cells were harvested at 60 h post-transduction.

The cell pellet from a 2 L culture was resuspended with 200 ml of hypotonic lysis buffer (20 mM KCl, 0.5 mM $MgCl_2$, 2 mM $CaCl_2$, 0.05 mg/ml DNase, and 10 mM Tris pH 8) for 25 min and then the lysate was spun at 39800 x g for 35 min to sediment crude membranes. The membrane pellet was mechanically homogenized and solubilized in extraction buffer (20 mM n-Dodecyl-β-D-Maltopyranoside (DDM), 4 mM cholesteryl hemisuccinate (CHS), 300 mM KCl, 2 mM $CaCl_2$, and 20 mM Tris pH 8) for 1.5 h. Solubilized membranes were clarified by centrifugation at 39800 x g for 35 min. The supernatant was applied to the GFP nanobody-coupled Sepharose resin (*64*), which was subsequently washed with 10 column volumes of wash buffer (0.5 mM DDM, 0.1 mM CHS, 150 mM KCl, 2 mM $CaCl_2$, and 20 mM Tris pH 8). The washed resin was incubated overnight with PreScission protease at a target protein to protease ratio of 40:1 (w/w) to cleave off GFP and release the protein from the resin. The protein was eluted with wash buffer, concentrated using an Amicon Ultra centrifugal filter (MWCO 100 kDa), and then injected onto a Superose 6 column (GE Healthcare) equilibrated with SEC buffer (0.5 mM DDM, 0.1 mM CHS, 150 mM KCl, 5 mM EGTA, and 20 mM Tris pH 8). Peak fractions were pooled and concentrated to ~5

mg/ml for EM grid preparation. To purify the channel complex in the Ca^{2+}-bound state, 2 mM $CaCl_2$ instead of EGTA was used in the SEC buffer. All buffers contained protease inhibitors (2 µg/ml leupepetin, 1 µg/ml pepstatin, 50 µg/ml benzamidine, 10 µg/ml aprotinin, and 1 mM AEBSF). All steps were performed at 4 °C.

Proteoliposome reconstitution and flux assay

1-palmitoyl-2-oleoyl-*sn*-glycero-3-phosphoethanolamine (POPE) and 1-palmitoyl-2-oleoyl-*sn*-glycero-3-phospho-(1'-*rac*-glycerol) (POPG) in chloroform were mixed at a 3:1 ratio (w/w), dried under an argon stream, and placed in a vacuum chamber overnight. Dried lipids were suspended by sonication in buffer containing 150 mM KCl, 20 mM Tris pH 8. DDM was mixed with the lipid suspension for 3 h at room temperature. The final DDM concentration was 15 mM and the lipid concentration 10 mg/ml. Purified SK/CaM protein in the presence of Ca^{2+} was added to the lipid/DDM mixture at a protein-to-lipid ratio of 1:100 (w/w). After 1 h at room temperature, SM-2 biobeads (Bio-Rad) were added to remove DDM, and the mixture was incubated at 4 °C overnight. Proteoliposome vesicles were collected and briefly sonicated prior to the assay. 0.5 µl vesicles were mixed with 39.5 µl flux assay buffer (150 mM NaCl, 2mM $CaCl_2$, 2 µM ACMA, 20 mM Tris pH 8). When indicated, 10 µM NS6180 or senicapoc was added to the flux assay buffer. Fluorescence was recorded every 5 seconds (λ_{EX} = 410 nm, λ_{EM} = 490 nm) using a plate reader (Tecan Infinite M1000). After the ACMA fluorescence stabilized, K^+ flux was initiated by addition of 1 µM CCCP (*21*). At the end of the assay, 4 µM valinomycin was added to release K^+ from all vesicles and yield a minimum baseline fluorescence. Note that there were dead times during t = 45–75 s and 225–255 s due to CCCP and valinomycin addition, respectively.

EM data acquisition

Aliquots of 3.5 µl purified SK/CaM complex sample were applied to glow-discharged Quantifoil R1.2/1.3 400 mesh Au grids. After 15 s, the grids were blotted for 1 s and plunged into liquid ethane using a Vitrobot Mark IV (FEI) operated at 22 °C and 100% humidity. The grids were loaded onto a 300 keV Titan Krios transmission electron microscope (FEI) with the K2 Summit detector (Gatan). Micrographs were recorded in super-resolution mode using SerialEM (*65*). Images have a calibrated physical pixel size of 1.03 Å (super-resolution pixel size of 0.515 Å) and a nominal defocus range of 1.2 to 2.3 µm. A dose rate of 8 electrons per pixel per second was used. The exposure time for each image was 10 s, with 0.2 s per frame. This gave a total cumulative dose of ~75 electrons per $Å^2$ (1.51 electrons per $Å^2$ per frame). Acquisition parameters are summarized in table S1.

Image processing

Super-resolution image stacks were gain-normalized, binned by 2 with Fourier cropping, and corrected for beam-induced motion using MotionCor2 (*66*). Contrast transfer function parameters were estimated from motion-corrected summed images without dose-weighting using GCTF (*67*). All subsequent processing was performed on motion-corrected summed images with dose-weighting. About 3,000 particles were manually picked and processed with reference-free 2D classification in RELION (*68*) to generate a template, which was used for particle picking using Gautomatch (written by Kai Zhang). Auto-picked particles were visually examined to remove false positives and were further cleaned up by multiple rounds of 2D classification.

For the Ca^{2+}-free state dataset, an *ab-initio* 3D model was generated from selected particles using cryoSPARC (*69*). Using this starting model, a consensus 3D refinement on selected particles

was run in RELION, followed by a 3D classification with a 1.8° angular sampling and local angular searches around the refined orientations (fig. S1C). The major class (36.5 % particles) had better secondary structure features and was further refined to 3.4 Å resolution (C4 symmetry imposed) or 3.9 Å (no symmetry imposed). To resolve the conformational heterogeneity of the CaM N-lobe, we performed a focused classification (fig. S3A). The particles after a consensus 3D refinement were first expanded according to the C4 point group (*31*). A soft mask covering only one subunit was applied to the reconstruction and signals outside the mask were subtracted from the experimental particles (*70*). The modified particles were subjected to 3D classification while keeping particle orientations fixed at values determined in the previous consensus refinement. This classification yielded three major classes that showed interpretable density for the CaM N-lobe (fig. S3A). We then conducted separate 3D refinements on the original, non-subtracted particles of these classes. The refinements were done with local angular searches around the refined orientations. In the last iteration of each refinement, a soft mask covering one subunit was applied and the refinement was continued until convergence.

For the Ca^{2+}-bound state dataset, a consensus 3D refinement was run on selected particles, followed by a 3D classification while keeping particle orientations fixed at values determined in the previous consensus refinement (fig. S4C). The major class (state I, 40.2 % particles) was subjected to particle polishing (*71*) and refined to 3.5 Å resolution (C4 symmetry imposed). The second major class (state II, 23.0 % particles) was also subjected to particle polishing, and further processed using cryoSPARC to refine to 4.7 Å resolution (C4 symmetry imposed).

The FSC curves were calculated with soft masks that exclude the detergent micelles and the effects of masking were corrected by the post-processing procedure in RELION (*72*). The reported resolutions were based on the FSC = 0.143 criterion (*73*) (figs. S1F and S4F, and table S1). Local resolutions of unfiltered density maps were estimated by Blocres with a kernel size of 17–17.5 (figs. S1E and S4E).

Model building

For the transmembrane domain, a *de novo* atomic model of a monomer was built in Coot (*74*) based on the consensus 3.4 Å Ca^{2+}-free state cryo-EM map. For the soluble domain, the CaM C-lobe, HA and HB helices from the crystal structure (PDB: 1G4Y) were docked into the maps using UCSF Chimera (*75*). The model was then manually adjusted in Coot. A tetramer model of the complex was obtained subsequently by applying a symmetry operation on the monomer. This tetramer model was refined using phenix.real_space_refine (*76*) with secondary structure restraints and Coot iteratively. The resulting Ca^{2+}-free SK/CaM channel structure, together with the CaM N-lobe from the crystal structure, was used as an initial model for the Ca^{2+}-bound structure. The Ca^{2+}-bound model was rebuilt and refined following the same procedure. The final Ca^{2+}-free structure includes human SK4 residues 10–123 and 142–386, and CaM residues 81–147. The final Ca^{2+}-bound structure includes human SK4 residues 9–123 and 142–386 and CaM residues 2–147. Residues whose side chains have poor density were modeled as alanines. For validation, FSC curves were calculated between the final models and EM maps (figs. S1F and S4F). The quality of final models was evaluated by MolProbity (*77*) and EMRinger (*78*) (table S1). The pore radii were calculated using HOLE (*79*). Figures were prepared using PyMOL (*80*) and Chimera.

Electrophysiological recording

Chinese hamster ovary K1 cells were cultured on coverslips placed in a 6-well plate containing DMEM/F-12 medium (Gibco) supplemented with 10% fetal bovine serum. The cells in each well

were transiently transfected with 2 μg SK4 DNA plasmid using Lipofectamine 3000 (Invitrogen) according to the manufacturer's instructions. After 36–60 h, the coverslips were transferred to a recording chamber containing the external solution (150 mM NaCl, 5 mM KCl, 1 mM $CaCl_2$, 10 mM glucose, and 10 mM HEPES pH 7.4). Borosilicate micropipettes (OD 1.5mm, ID 0.86 mm, Sutter) were pulled and fire polished to 2–5 MΩ resistance. For inside-out recordings, the pipette solution was 160 mM KCl, 1 mM $CaCl_2$, and 10 mM HEPES pH 7.4. The bath solution was 150 mM KCl, 5 mM EGTA, 1 mM ATP, 1 mM $MgCl_2$, and 10 mM HEPES pH 7.4. To yield a final free Ca^{2+} concentration of 10 μM, 5 mM $CaCl_2$ was added to the bath solution when indicated based on the program MAXCHELATOR (http://maxchelator.stanford.edu). 2 mM MTSES (Toronto Research Chemicals) was freshly prepared immediately before application and added directly into the bath solution. Inside-out recordings were obtained at room temperature (~23 °C) using an Axopatch 200B amplifier, a Digidata 1550 digitizer and pCLAMP software (Molecular Devices). The patches were held at −80 mV and the recordings were low-pass filtered at 1 kHz and sampled at 20 kHz. Statistical analyses were performed using GraphPad Prism.

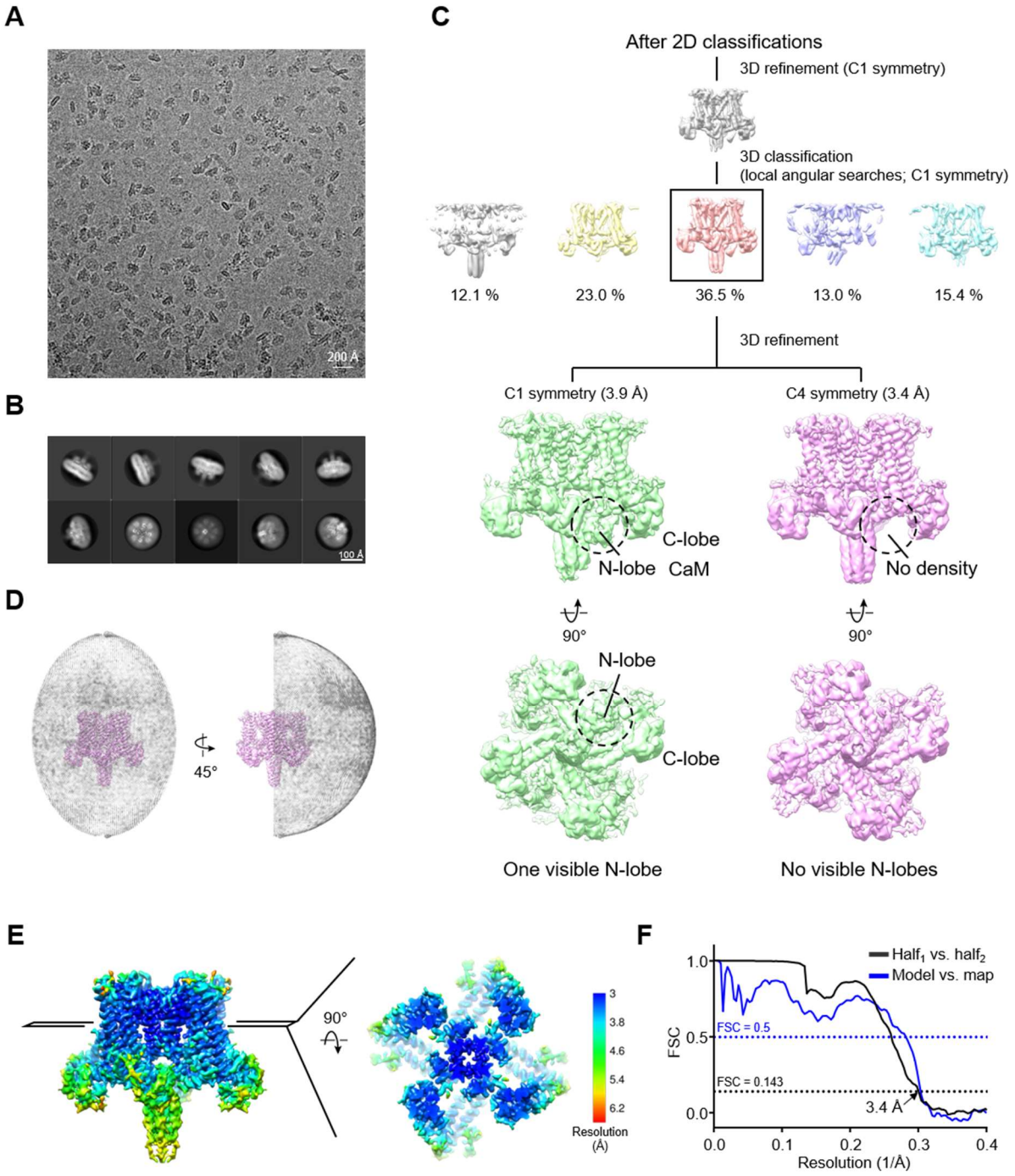

Fig. S1. Cryo-EM reconstructions of the Ca^{2+}-free SK/CaM channel complex.
(**A**) A representative raw micrograph of the SK/CaM channel complex in the absence of Ca^{2+}. (**B**) Selected 2D class averages. (**C**) Summary of image processing for the Ca^{2+}-free state dataset. Only one CaM N-lobe has defined density if no symmetry is imposed during reconstruction (green), whereas none of the CaM N-lobes have defined density if C4 symmetry is imposed (pink). (**D**) Euler angle distribution of particles for the final 3D reconstruction. The radii of gray spheres are proportional to the number of particles assigned to that specific orientation. (**E**) Local resolution

of density map estimated by Blocres. (**F**) Fourier shell correlation (FSC) curves: half map 1 versus half map 2 (black), model versus summed map (blue).

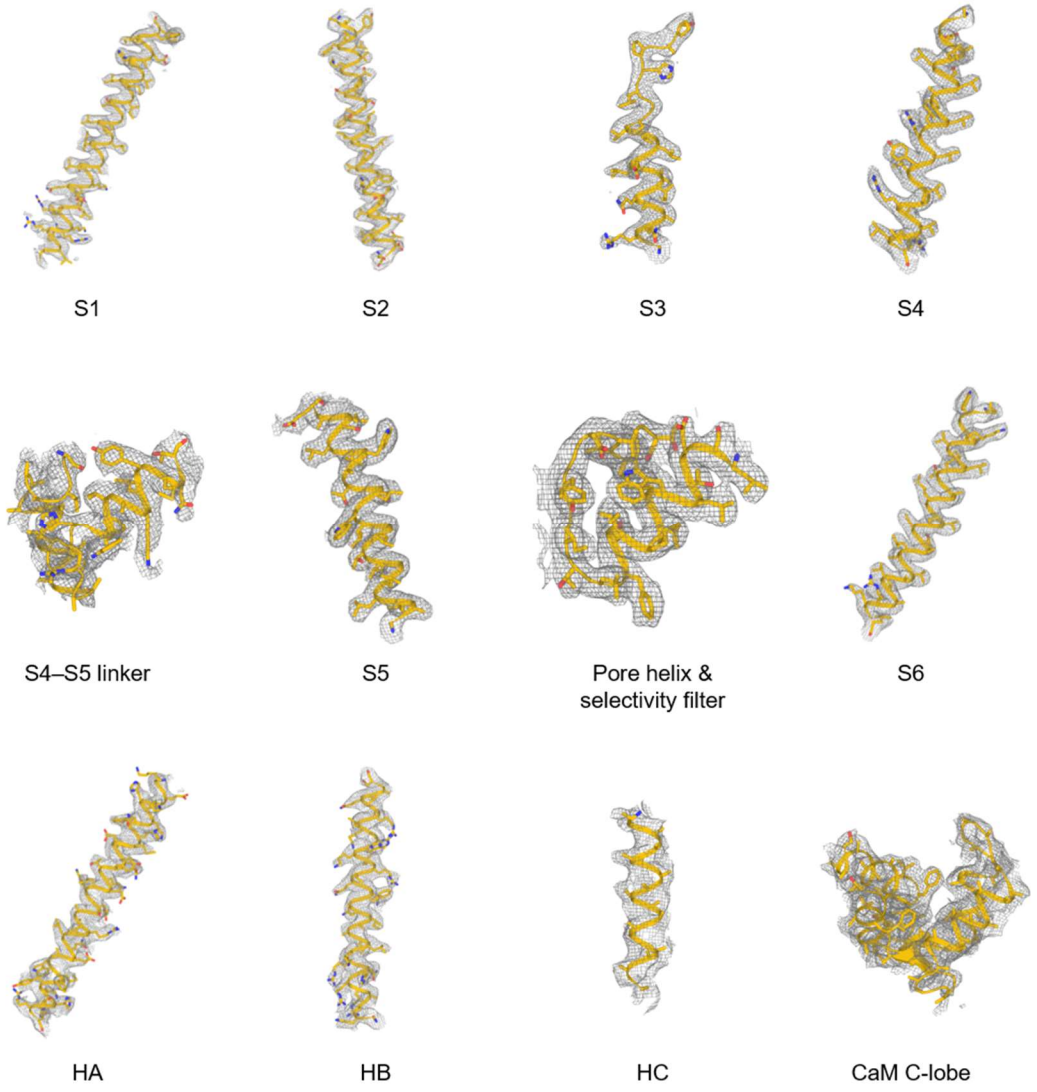

Fig. S2. Representative cryo-EM densities of the Ca^{2+}-free SK/CaM complex.

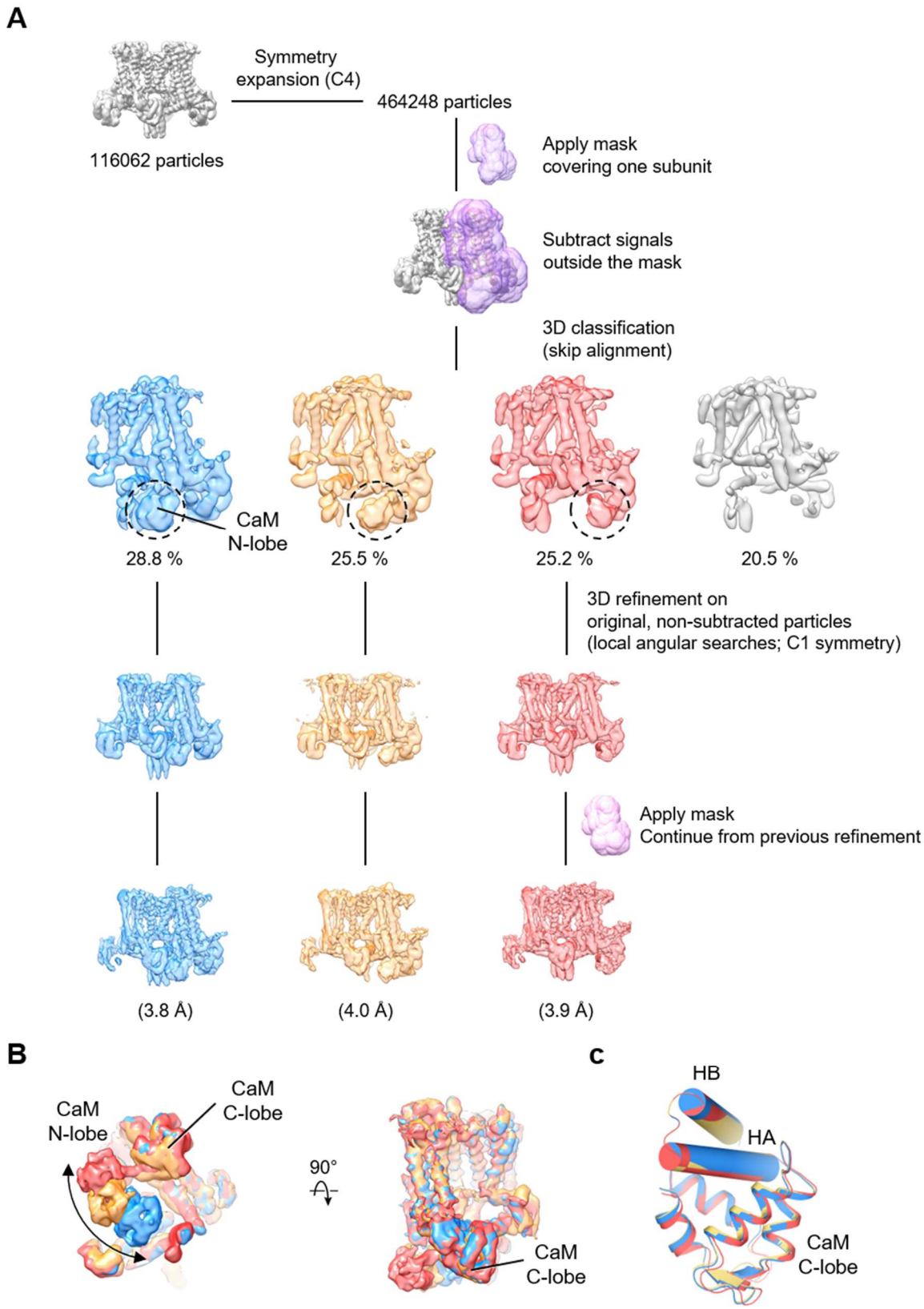

Fig. S3. Focused 3D classification/refinements on the Ca^{2+}-free SK/CaM complex.

(**A**) Summary of image processing to resolve the conformational heterogeneity of the CaM N-lobe. (**B**) Comparison of the three CaM conformations. While N-lobes display dramatic rearrangements, C-lobes only have subtle movements. For clarity, only density within the mask is shown. (**C**) Structural comparison of CaM C-lobes. Structures are aligned using HA and HB.

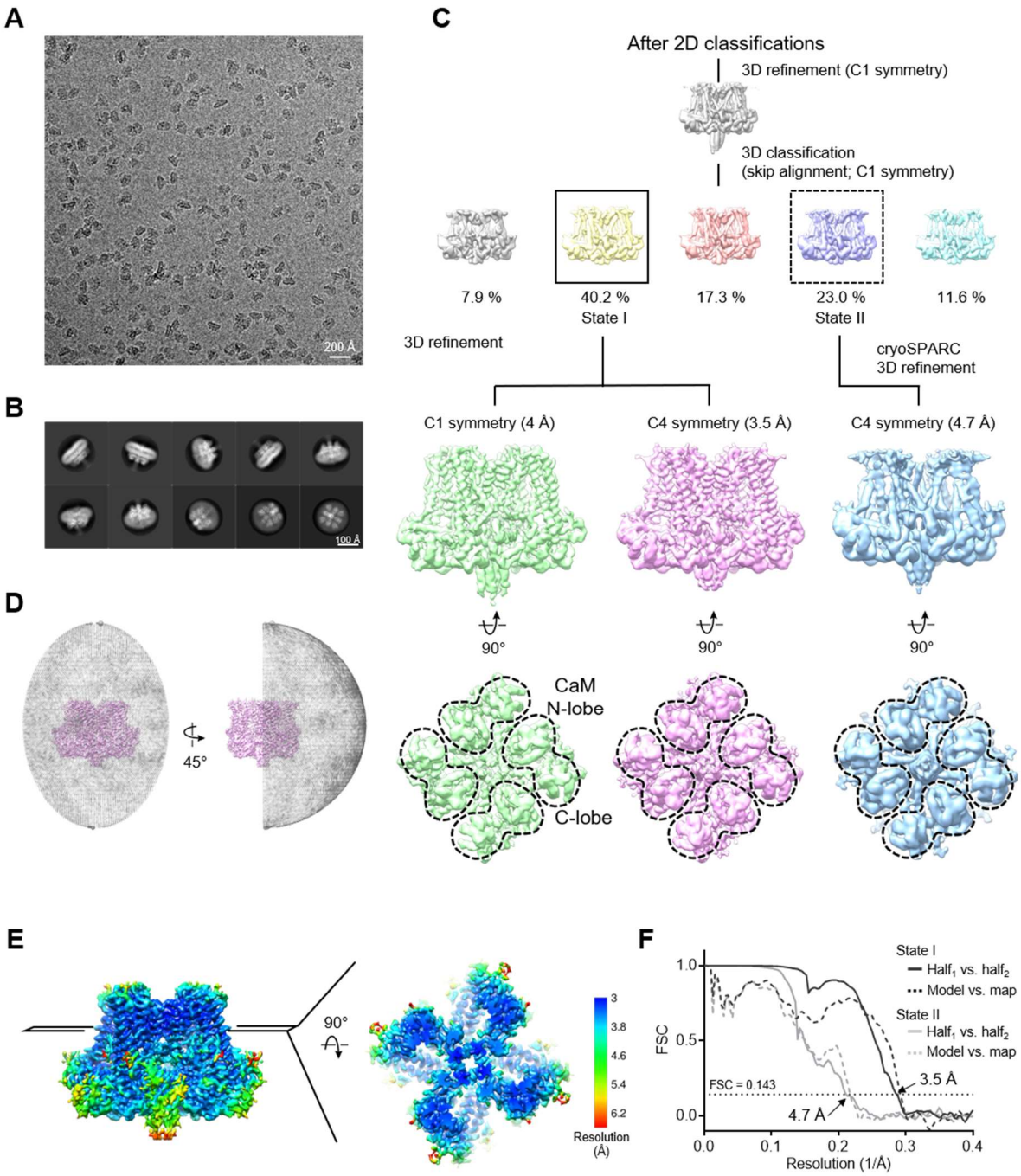

Fig. S4. Cryo-EM reconstructions of the Ca^{2+}-bound SK/CaM channel complex.
(**A**) Representative raw micrograph of the SK/CaM channel complex in the presence of Ca^{2+}. (**B**) Selected 2D class averages. (**C**) Summary of image processing for the Ca^{2+}-bound state dataset. Note that the channel complex remains 4-fold symmetric even if no symmetry is imposed during reconstruction (green). (**D**) Euler angle distribution of particles for the final 3D reconstruction. The radii of gray spheres are proportional to the number of particles assigned to that specific orientation. (**E**) Local resolution of density map estimated by Blocres. (**F**) Fourier shell correlation (FSC) curves: half map 1 versus half map 2 (solid lines), model versus summed map (dashed lines).

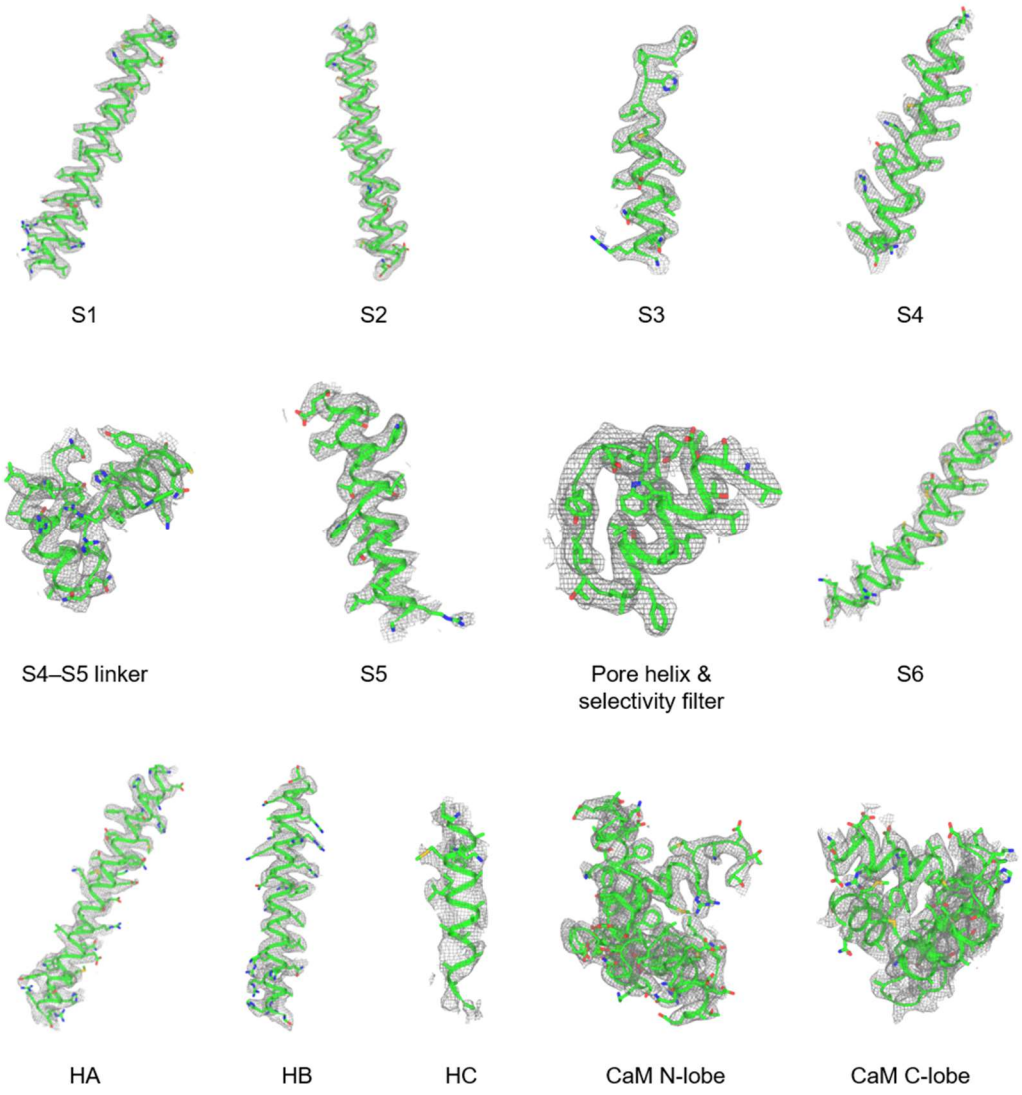

Fig. S5. Representative cryo-EM densities of the Ca^{2+}-bound SK/CaM complex.

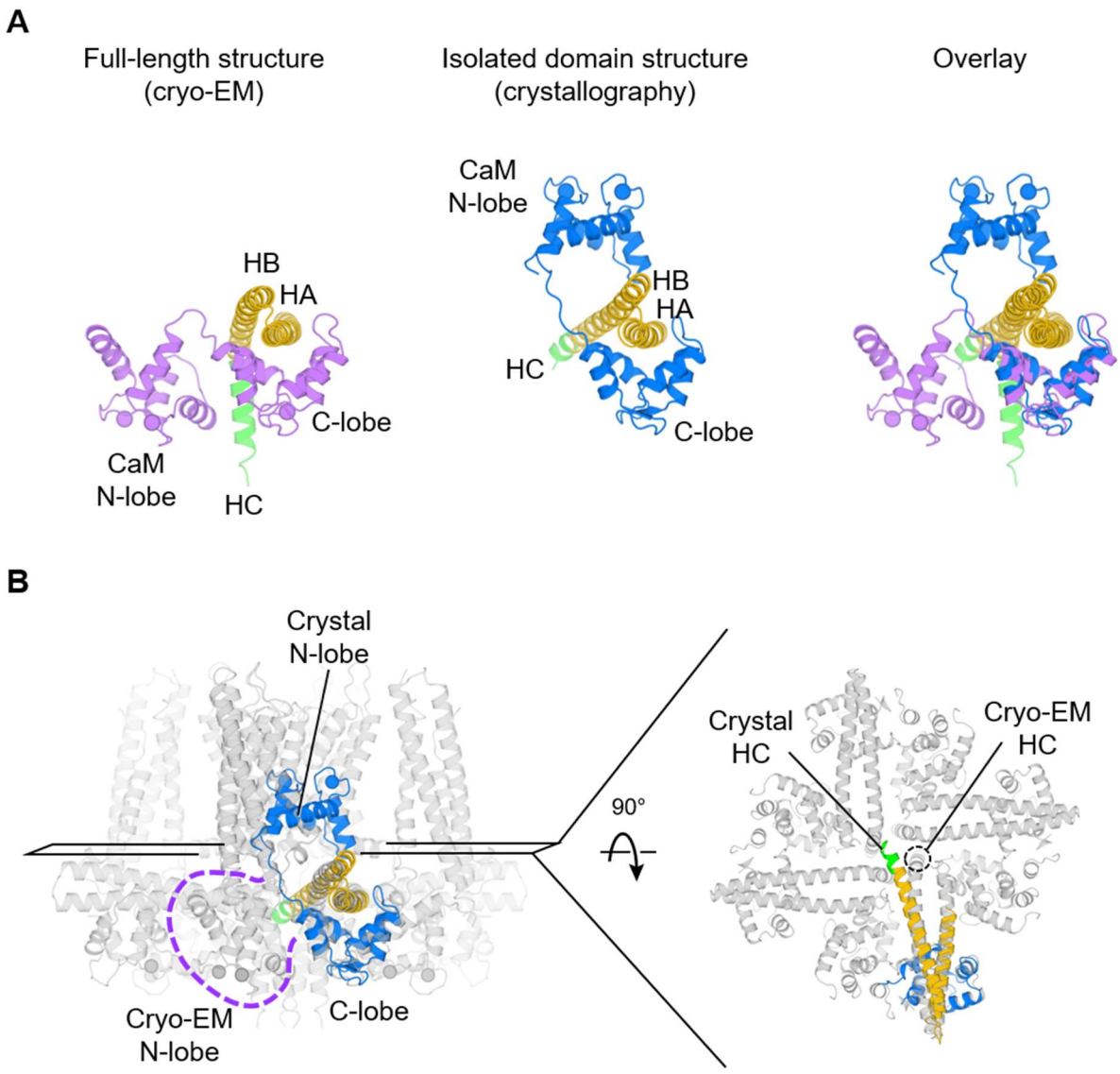

Fig. S6. Comparison of the full-length Ca^{2+}-bound SK/CaM complex structure and the isolated domain structure.

(**A**) Comparison of HA–HC helices/CaM in the full-length structure and in the isolated domain crystal structure (PDB: 1G4Y). Structures are aligned based on the CaM C-lobe. For clarity, only one pair of HA–HC helices/CaM from the crystal structure is shown. (**B**) Overlay of the full-length structure and the isolated domain structure. Note that the CaM N-lobe in the crystal structure (blue) adopts a conformation that would clash with the transmembrane domains of the channel.

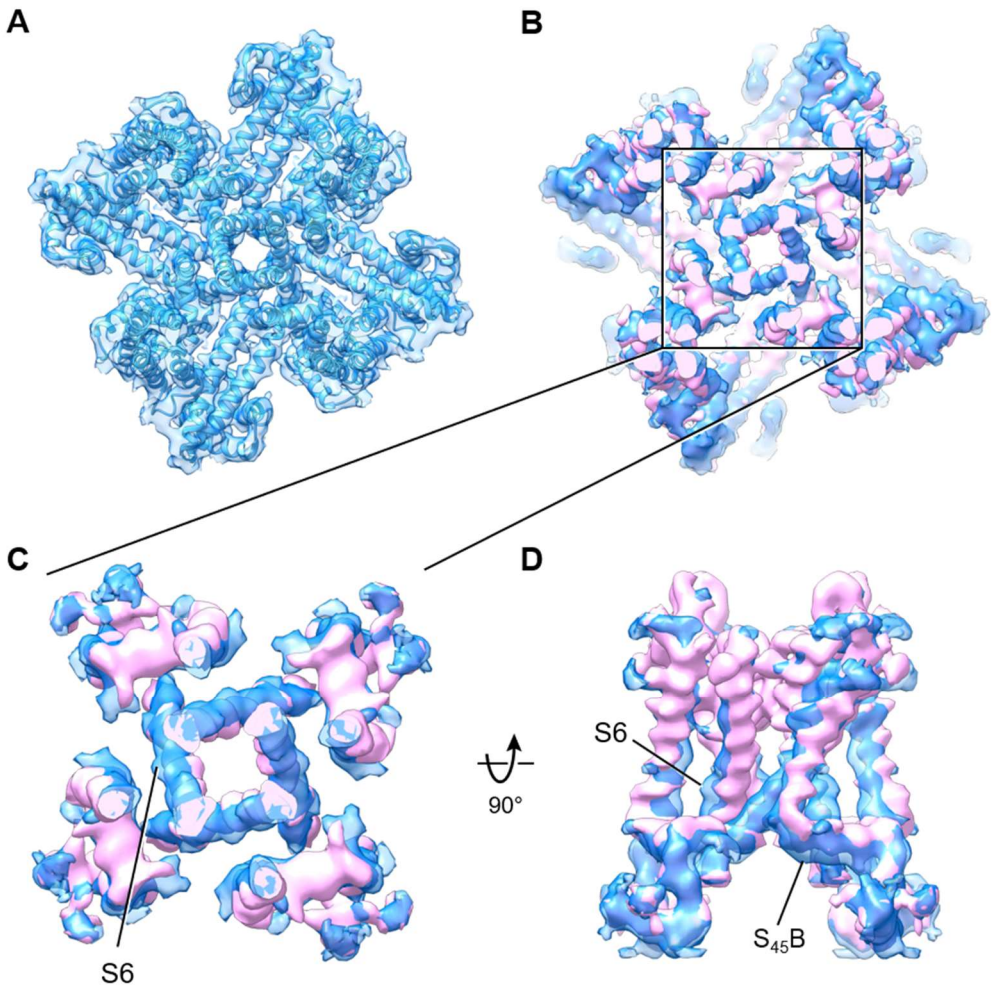

Fig. S7. Comparison of the SK/CaM activated state I and state II.
(**A**) Structure of the SK/CaM channel complex in the activated state II. A top-down view is shown from the middle of the membrane, near the pore constriction. (**B** to **D**) Overlay of the state I (pink) and the state II (blue). The density map of the state I is low-passed filtered to 4.7 Å resolution to match the resolution of the state II. In state II, the pore, formed by the S6 helices, expands more (C) and $S_{45}B$ moves further down towards the cytoplasm (D).

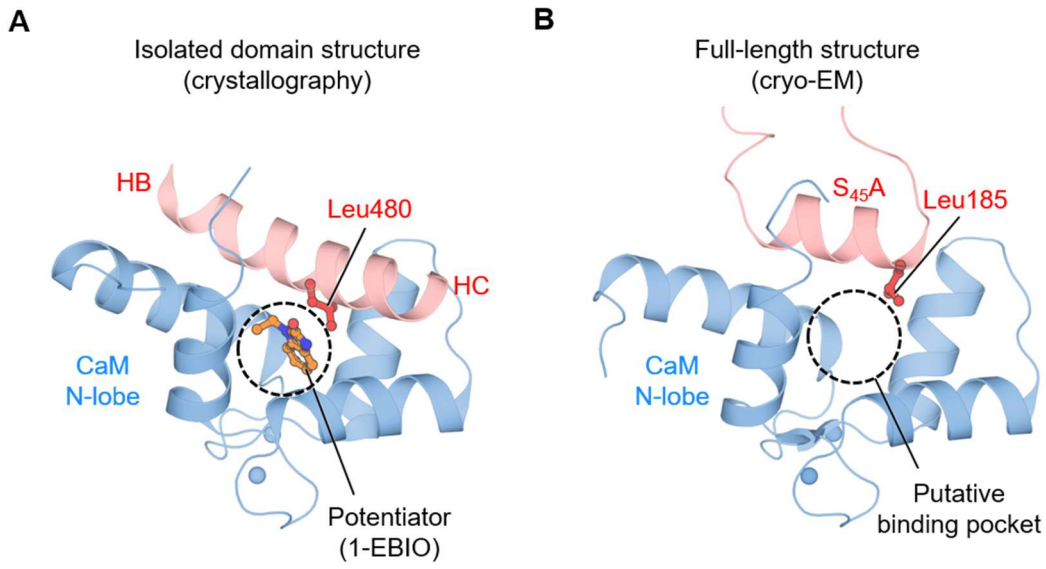

Fig. S8. Potential modulator-binding pockets in the Ca^{2+}-bound SK/CaM channel complex. (**A**) SK channel potentiator EBIO-1 in complex with SK2 fragments/CaM (PDB: 4G28). In the crystal structure, Leu480 mediates EBIO-1 binding. (**B**) Potential modulator-binding pocket formed by $S_{45}A$ and the CaM N-lobe. In our full-length structure, Leu185 occupies a similar location as the Leu480 of the crystal structure. We propose that in the native channel complex, Leu185 interacts with modulators and, together with the CaM N-lobe, forms a binding pocket for modulators.

	Ca^{2+}-free	Ca^{2+}-bound	
Data acquisition			
Microscope	Krios	Krios	
Voltage (kV)	300	300	
focus range (μm)	−1.2 to −2.3	−1.2 to −2.3	
Pixel size (Å)	1.03	1.03	
Total electron dose ($e^-/Å^2$)	75	75	
Exposure time (s)	10	10	
Reconstruction			
Particle number	42422	91511	52056
Resolution (unmasked, Å)	4.06	4.01	7.36
Resolution (masked, Å)	3.39	3.51	4.69
Rms deviations			
Bond length (Å)	0.021	0.022	0.006
Bond angle (°)	0.891	0.879	1.020
Ramachandran plot			
Favored (%)	95.7	96.0	96.5
Allowed (%)	4.3	4.0	3.5
Validation			
EMRinger score	3.41	2.52	N.D.
MolProbity score	1.24 (100^{th})	1.19 (100^{th})	1.53 (100^{th})
Clashscore	1.8 (100^{th})	1.63 (100^{th})	5.64 (100^{th})

Table S1. Summary of data acquisition parameters and refinement statistics.

Movie S1. Activation mechanism of the SK/CaM channel complex.
An animation of the CaM movement and conformational changes of the SK channel upon Ca^{2+} binding. The positions of CaM N-lobes in the Ca^{2+}-free state can not be accurately assigned in the current study. We tentatively docked the X-ray structure of the Ca^{2+}-free CaM N-lobe (PDB: 4LZX) into the corresponding cryo-EM densities for animation purpose.